Journal of Electrostatics 71 (2013) 179–184

Contents lists available at SciVerse ScienceDirect

Journal of Electrostatics

journal homepage: www.elsevier.com/locate/elstat

Non-thermal plasma generation by using back corona discharge on catalyst

Fada Feng, Lingling Ye, Ji Liu, Keping Yan*

Key Laboratory of Biomass Chemical Engineering of Ministry of Education, Industrial Ecology and Environment Research Institute, Department of Chemical and Biological Engineering, Zhejiang University, Hangzhou 310028, PR China

ARTICLE INFO

Article history:
Received 1 September 2012
Received in revised form
21 November 2012
Accepted 29 November 2012
Available online 10 December 2012

Keywords:
Back corona
VOCs
Catalysis
Non-thermal plasma

ABSTRACT

This paper discusses a novel plasma catalysis generation method based on back-corona discharge along porous catalyst bed reactor. The reactor consists of a high-voltage needle electrode, one floated mesh electrode, one catalyst bed and one grounded mesh electrode. Typical plasma current density is 11.88 μA/cm^2. It can be used for ozone generation and volatile organic compounds decomposition. By using a home-made AgMnOx/Al_2O_3-1 catalyst, 90% of toluene is removed at the specific plasma energy density of 123 J/L. At the same time, aerosol byproducts are collected and then decomposed on the catalyst bed. Moreover, the catalyst is regenerated because of the back-corona discharge.

1. Introduction

Plasma is a partially or fully ionized gas composed of electrons, highly excited atoms, ions, radicals, and molecules. For non-thermal plasma, only the electrons are energized, the bulk gases and ions are not significantly heated [1]. Chemical reactions in the plasmas are mainly initiated by active electrons. A few examples are pollution emission control [2–4], chemical synthesis [5,6], surface treatment and disinfection [7,8]. Plasma-assisted catalysis has the potential to enhance global reaction rate, improve the reaction selectivity and increase energy utilization efficiency [9]. There are several techniques to generate non-thermal plasmas, such as DC streamer corona discharge, pulsed streamer corona discharge, dielectric barrier discharge (DBD), electron beam irradiation and microwave discharge. The streamer corona and DBD techniques are two of the most commonly used electrical discharge methods at atmospheric pressure. With regard to plasma energy density per unit reactor volume and system pressure drop across the reactor, the two techniques show very different characteristics.

Back corona discharge phenomena are often observed in electrostatic precipitators. When the plate electrode covered with high resistivity dielectric layer, electric charges emitted by the point electrode accumulate on the surface and within the dielectric layer. As a result, electrical breakdown of the dielectric layer may occur. The discharge can also be used as a plasma generation method for inducing chemical reactions [10]. Its fundamentals have been widely investigated in terms of voltage and current characteristics [11–18]. Examples are for ozone generation, diesel exhaust control, and hydrocarbon gaseous decomposition [19–22].

This paper presents a novel plasma catalysis generation method based on back corona discharge along porous alumina catalyst, point and mesh electrodes. The plasmas are generated by negative DC discharge in a needle-mesh precipitator and back corona discharge is generated with a mesh-catalyst-mesh hybrid electrodes. Home-made MnOx and Ag–MnOx catalysts are used for experiments. The discharge voltage–current characteristics, pulse current characteristics and ozone concentration are used to evaluate the technique. At the same time, toluene decomposition and catalyst regeneration are experimentally investigated in order to develop a cost-effective plasma generation method.

2. Experimental setup

Fig. 1 shows a schematic diagram of the experimental setup for plasma catalysis generation. Two forms of discharge configuration are used to study back corona discharge, i.e., needle-plate and needle-mesh-mesh. For the needle-plate configuration (Fig. 1a), alumina particles or porous alumina are placed above the stainless steel plate with a diameter of 100 mm. For the plasma catalysis reactor (Fig. 1b), needle-mesh-mesh electrodes are used for volatile organic compounds (VOCs) removal. The middle mesh electrode is floated on the catalyst. All of them are placed inside a glass tube

* Corresponding author. Tel.: +86 571 88210786; fax: +86 571 88210340.
E-mail address: kyan@zju.edu.cn (K. Yan).

0304-3886/$ – see front matter © 2012 Elsevier B.V. All rights reserved.
http://dx.doi.org/10.1016/j.elstat.2012.11.034

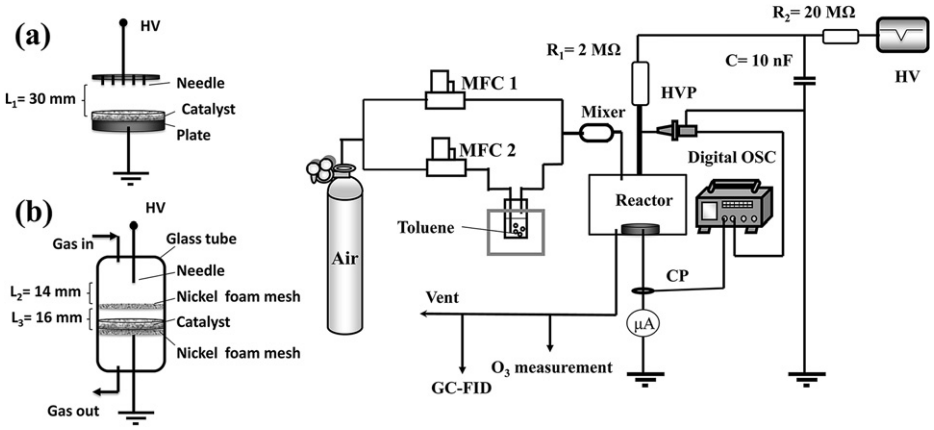

Fig. 1. Schematic diagram of experimental setup.

with an inner diameter of 40 mm. The two mesh electrode diameters are 38 mm. The nickel foam mesh electrodes have pores per inch (PPI) of 110. The discharge is powered by a negative DC high-voltage power source.

Alumina particles and porous alumina are made from pseudo-boehmite. The pore sizes of the porous alumina are 1.25 mm, 1 mm, and 0.76 mm, respectively. The home-made catalysts of AgMnO*x*, MnO*x*, MnO*x*/Al_2O_3 and AgMnO*x*/Al_2O_3 are prepared by the methods of oxydoreduction precipitation, impregnation, and surface coating method, respectively. Their resistivities are evaluated at temperature of 120 °C.

The experiments are carried out in dry air at atmospheric pressure and ambient temperature. For VOCs removal, the initial toluene concentration in the mixed air is 409 mg/m^3 with a total gas flow rate of 500 mL/min.

The negative DC voltage is measured with a voltage probe (P6015A, Tektronix). The average and pulse currents are measured with a DC Amperemeter (C31/1-μA, Shanghai) and a current probe (TCP202, Tektronix), respectively. The plasma photographs are taken by a digital camera (Canon, EOS 7D). Gas samples are analyzed by a gas chromatograph (GC-9750, Fuli). The ozone concentration is measured by iodometric titration.

3. Results and discussion

3.1. Back corona

For conventional electrostatic precipitator, when the apparent dust resistivity ρ_d becomes higher than 5×10^8 Ωm, back corona can be generated with a larger corona current density [23]. Our home-made catalysts have a resistivity of 8.3×10^{10} Ωm for present work in order to generate plasma effectively.

Onset glow discharge is observed on the alumina layer at the applied voltage of 22 kV for needle-plate configuration (Fig. 2a). The glow becomes steady streamer corona with increasing the applied voltage (Fig. 2b). At 40 kV, the discharge current rises to 200 μA, which is four times higher than the current value obtained without using the layer. As shown in the Fig. 3, the pulse current of back corona discharge can be detected by the current probe. When the breakdown streamer occurs, the alumina particles are spattered from the layer and moved towards the needle, and after that the craters remained (Fig. 4). The erosion of catalyst particles can be eliminated by using a forming catalyst.

In comparison with point-plate corona discharge illustrated in Fig. 5a, Fig. 5b shows the back corona discharge generated by placing the porous alumina on the plate. For single needle discharge, the back corona discharge occurs only in part of the catalyst bed because of the non-uniform field strength. Multi-needle-plate can be used to generate large area plasma in porous alumina (Fig. 5c). The proposed new method is to use two parallel metal mesh electrodes with porous catalysts in between. Corona discharge is generated between the point and the floated mesh electrode, and non-thermal plasma is generated inside the catalyst bed between the two metal mesh electrodes. Because one electrode is floated, the plasma current density is automatically controlled by the corona discharge. And very uniform plasma can be generated for chemical reactions. Typical plasma photo is shown in Fig. 5d.

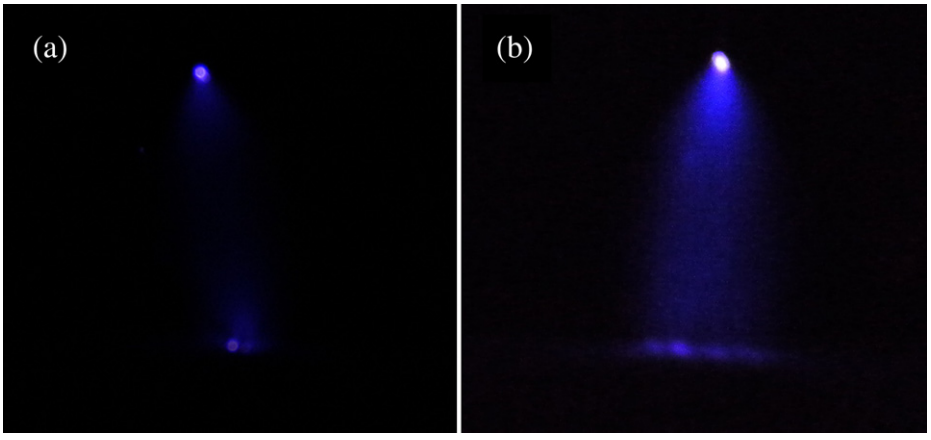

Fig. 2. Stationary discharges photographs with alumina particles. (a) Onset corona, (b) steady corona.

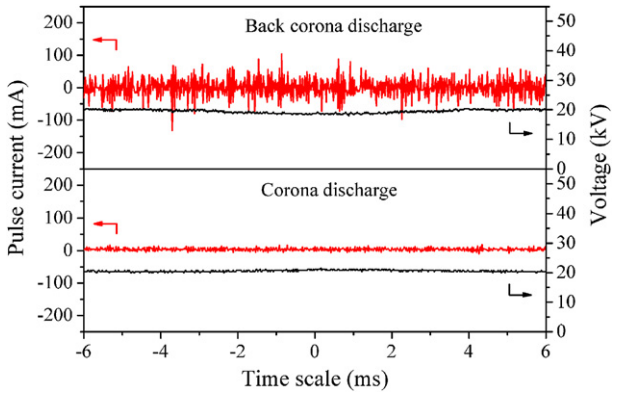

Fig. 3. Time-resolved discharge currents with and without back corona discharges.

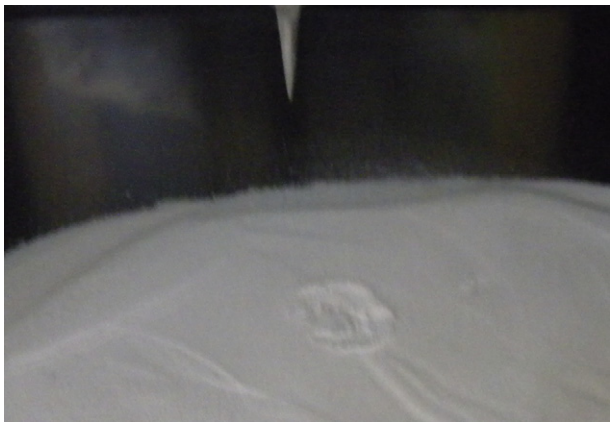

Fig. 4. Photograph of discharged induced catalyst erosion.

3.2. Plasma generation

The electric charges emitted from the needle electrode are redistributed on the nickel floated-electrode. Then the charges are accumulated on the alumina surface to raise the electric field across the alumina layer till breakdown occurs inside the catalyst bed to balance the current flow.

Fig. 6 shows the discharge current–voltage characteristics with various pore sizes of alumina materials but not loaded catalyst. In comparison with without back-corona discharge, the discharge current density is increased significantly with the applied voltage. It is obvious that the small pores alumina gives the largest discharge current. For example, at the applied voltage of 19 kV, the discharge current densities for alumina with pore sizes of 0.76 mm, 1 mm, and 1.25 mm are about 11.88 μA/cm^2, 9.88 μA/cm^2 and 7.94 μA/cm^2, respectively. For big pore size alumina, the surface cannot be charged effectively. As observed [24], however, if the pore size is very small (<1 μm), the discharge is only on the dielectric surface.

When using MnO*x*-1 and MnO*x*-1.25 catalysts, the discharge current densities become much higher (Fig. 7). Fig. 8 and Fig. 9 show typical corona images without and with catalysts loaded, respectively. With MnO*x*/Al_2O_3 and AgMnO*x*/Al_2O_3 catalysts, back corona discharge plasma can be easily generated for inducing chemical reactions (Fig. 9c and d).

3.3. Ozone generation

Porous alumina with and without active components are used to evaluate the generation of ozone in this system. Fig. 10 shows that the ozone concentration via the discharge current density. It is almost lineally dependent on the plasma current density, which in fact is a very cost-effective method to control the plasma density. For the unloaded porous alumina, the ozone concentration is significantly higher than that with loaded porous alumina. For example, at the same discharge current density of 10.58 μA/cm^2, the ozone concentrations with Al_2O_3-1 and AgMnO*x*/Al_2O_3-1 are about 1008 mg/m^3 and 424 mg/m^3, respectively.

It is well known that alumina has a low activity for ozone decomposition. In contrast, AgMnO*x* is an active catalyst for ozone decomposition. The ozone generated in discharge is partly decomposed on catalysts.

3.4. Toluene decomposition

The decomposition of toluene mainly consists of two steps: (1) fast stage plasma oxidation to partially convert toluene to aerosols and intermediate byproducts, and (2) by-products collection and

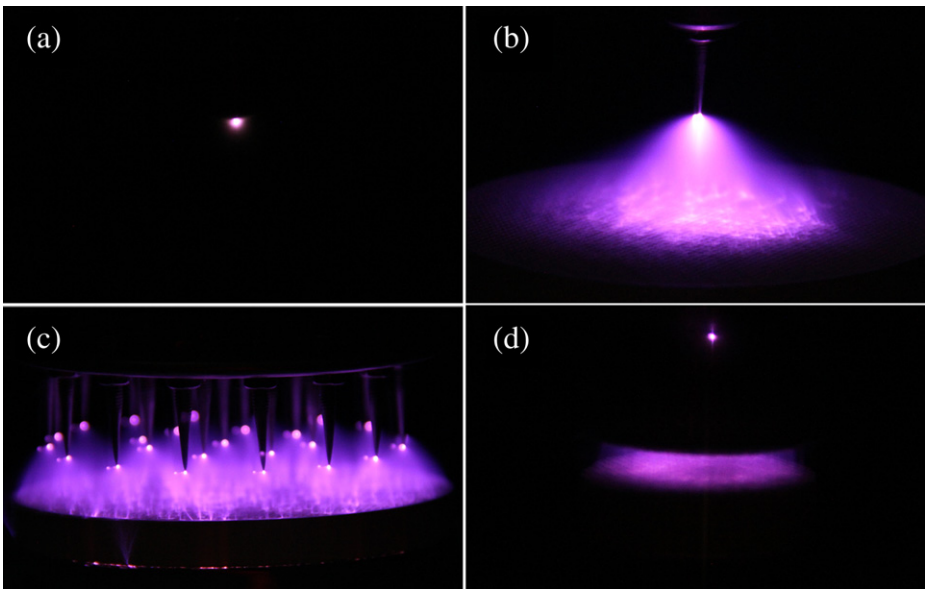

Fig. 5. Photographs of discharges with various electrodes at the applied voltage of 19 kV. Needle-plate electrode for (a) negative corona discharge, and (b) porous alumina (Φ100 mm); multi needle-plate electrode for (c) porous alumina (Φ100 mm); needle-mesh-mesh electrode for (d) porous alumina (Φ38 mm).

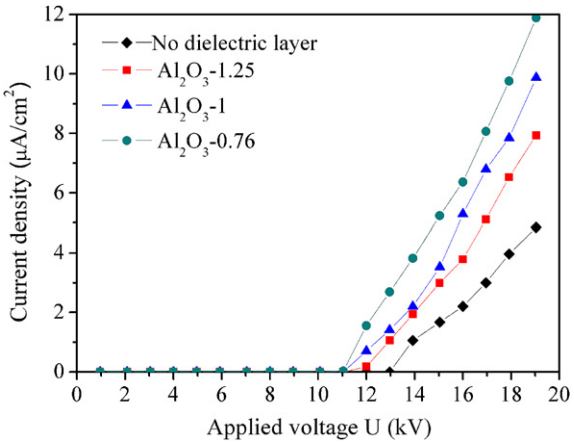

Fig. 6. Current–voltage characteristics with unloaded porous alumina.

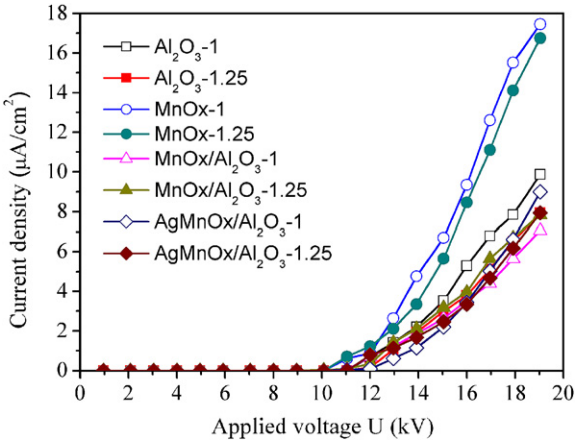

Fig. 7. Current–voltage characteristics with different catalysts.

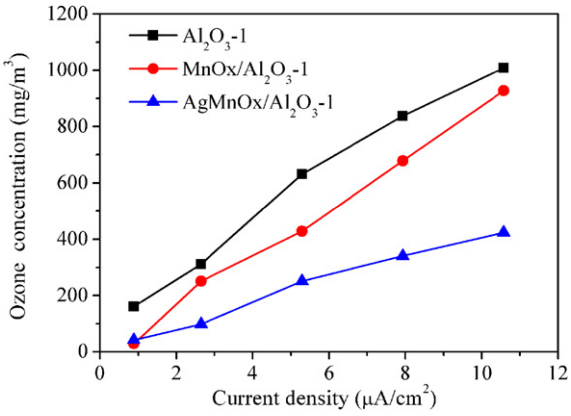

Fig. 10. The relationship between the current density and ozone concentration.

further oxidation on porous alumina catalyst bed. Fig. 11 and Fig. 12 show the toluene removal efficiency and ozone concentration, respectively. The toluene removal efficiency increases with the specific plasma input energy. The porous alumina loaded catalyst benefits toluene decomposition. For AgMnOx/Al_2O_3-1 catalyst, 90% and 95% toluene removal efficiency is observed at the specific input energy of 123 J/L and 286 J/L, respectively.

In the corona discharge region, the toluene is converted to aerosols. Then the charged aerosols can be collected easily on the catalyst where the back corona discharge plasma is generated. At a relative low current back corona discharge, the aerosols collected on the catalyst bed cannot be completely decomposed. Fig. 13 shows the aerosols collected on the AgMnOx/Al_2O_3 catalyst at the specific input energy of 123 J/L.

3.5. *Catalyst regeneration*

When back corona discharge occurs, the plasma is directly generated on the catalyst and short-lived active species generated

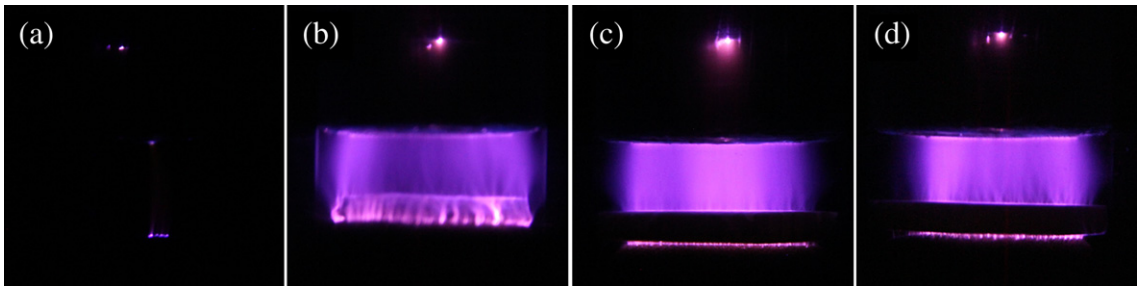

Fig. 8. Photographs with unloaded porous alumina at the applied voltage of 19 kV. (a) Without dielectric layer, (b) Al_2O_3-0.76, (c) Al_2O_3-1, (d) Al_2O_3-1.25.

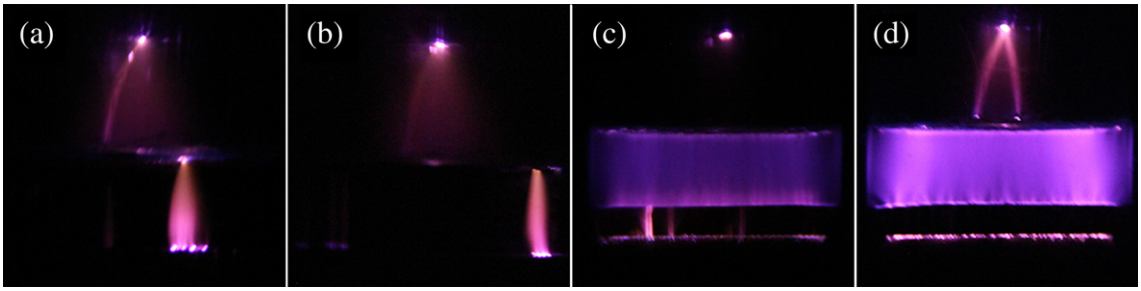

Fig. 9. Photographs with porous alumina loaded with different catalysts at the applied voltage of 19 kV. (a) MnOx-1, (b) MnOx-1.25, (c) MnOx/Al_2O_3-1, and (d) AgMnOx/Al_2O_3.

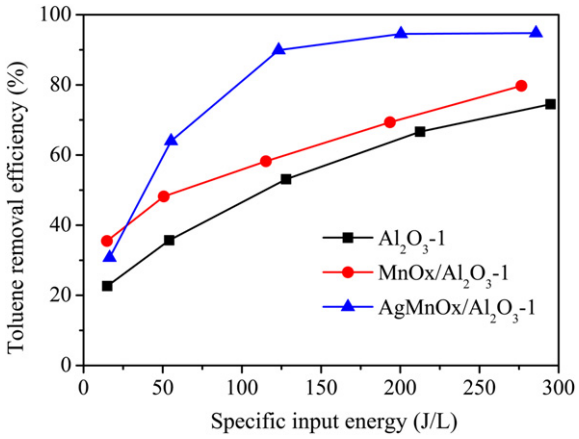

Fig. 11. The removal efficiency of toluene via the specific energy.

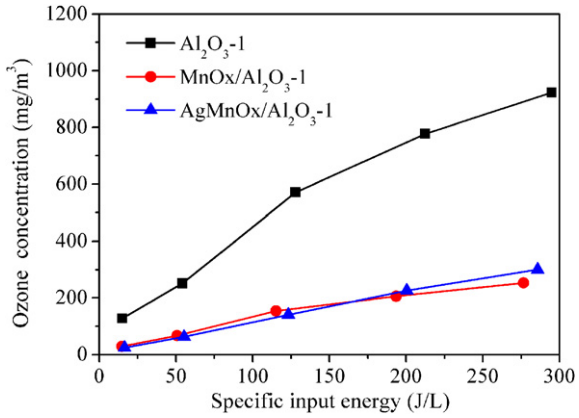

Fig. 12. The ozone byproduct via the specific input energy.

in discharge are used in situ for the catalyst regeneration. In fact, the deactivated catalyst is used as a dielectric layer for generation of the back corona. As an example, Fig. 14 shows the regeneration of the deactivated $MnOx/Al_2O_3$ catalyst that used for decomposition of ozone and toluene. At the discharge current density of 7 $\mu A/cm^2$,

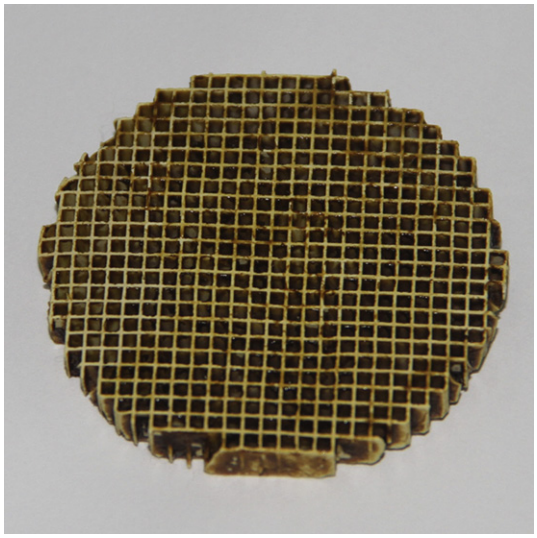

Fig. 13. Photographs of aerosols collected on the catalyst.

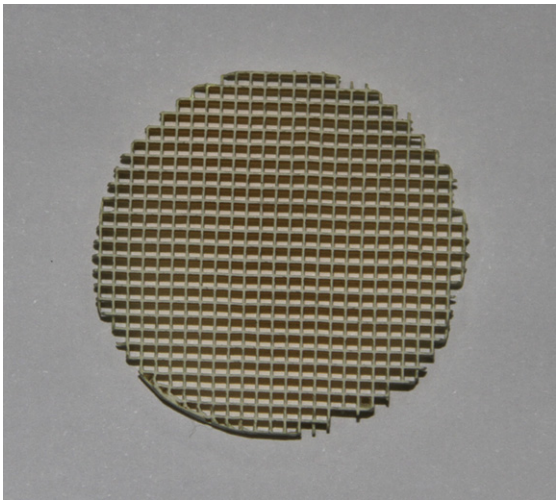

Fig. 14. Photograph of catalyst after regeneration.

the $MnOx/Al_2O_3$ catalyst is treated for 6 min in air. Its ozone decomposition efficiency increases from 35% before regeneration to 100% after treatment, with the condition of the concentration of ozone and toluene of 140 mg/m^3 and 42 mg/m^3, respectively.

4. Conclusions

The proposed plasma method consists of one floated mesh electrode, two connected electrodes and a catalyst bed. It is very effective for inducing gaseous oxidation, aerosol collection and oxidation. Its chemical reactivity in terms of ozone generation is linearly dependent on the plasma current density. In contrast to ozone production, VOCs decomposition efficiency is improved when less ozone is generated. With our home-made $AgMnOx/Al_2O_3$ catalysts, both VOCs and its byproduct aerosols can be effectively decomposed in air. Moreover, the catalysts can be effectively regenerated on site.

Acknowledgment

This work was supported financially by the Natural Science Foundation of China (No. 21006092).

References

[1] H. Winands, K.P. Yan, S.A. Nair, G. Pemen, B. van Heesch, Evaluation of corona plasma techniques for industrial applications: HPPS and DC/AC systems, Plasma Process. Polym. 2 (3) (2005) 232–237.
[2] J.S. Chang, Physics and chemistry of plasma pollution control technology, Plasma Sources Sci. T 17 (0450044) (2008).
[3] J. Jolibois, K. Takashima, A. Mizuno, Application of a non-thermal surface plasma discharge in wet condition for gas exhaust treatment: NO*x* removal, J. Electrostat. 70 (3) (2012) 300–308.
[4] F.M. Huang, L. Chen, H.L. Wang, T.Z. Feng, Z.C. Yan, Degradation of methyl orange by atmospheric DBD plasma: analysis of the degradation effects and degradation path, J. Electrostat. 70 (1) (2012) 43–47.
[5] H.J. Gallon, X. Tu, M.V. Twigg, J.C. Whitehead, Plasma-assisted methane reduction of a NiO catalyst-low temperature activation of methane and formation of carbon nanofibres E-5712-2011, Appl. Catal. B Environ. 106 (3–4) (2011) 616–620.
[6] M. Meyyappan, Plasma nanotechnology: past, present and future, J. Phys. D Appl. Phys. 44 (17400217) (2011).
[7] A. Simon, O.E. Dinu, M.A. Papiu, C.D. Tudoran, J. Papp, S.D. Anghel, A study of 1.74 MHz atmospheric pressure dielectric barrier discharge for non-conventional treatments, J. Electrostat. 70 (3) (2012) 235–240.
[8] K. Vasilev, S.S. Griesser, H.J. Griesser, Antibacterial surfaces and coatings produced by plasma techniques, Plasma Process. Polym. 8 (11) (2011) 1010–1023.
[9] J.C. Whitehead, Plasma catalysis: a solution for environmental problems E-5712-2011, Pure Appl. Chem. 82 (6) (2010) 1329–1336.

[10] T. Czapka, Back-corona discharge phenomenon in the nonthermal plasma system, IEEE T. Plasma Sci. 39 (11SIPart 1) (2011) 2242–2243.
[11] S. Masuda, A. Mizuno, Initiation condition and mode of back discharge, J. Electrostat. 4 (1) (1977) 35–52.
[12] S. Masuda, A. Mizuno, Flashover measurements of back discharge, J. Electrostat. 4 (3) (1978) 215–231.
[13] S. Masuda, A. Mizuno, M. Akimoto, Effects of gas composition on sparking characteristics of back discharge—preliminary study, J. Electrostat. 6 (4) (1979) 333–347.
[14] E. Rajch, A. Jaworek, T. Czech, M. Lackowski, Spectroscopic studies of back-discharge, Czech. J. Phys. 54 (Part 4) (2004) C772–C777.
[15] T. Czech, A.T. Sobczyk, A. Jaworek, Optical emission spectroscopy of point-plane corona and back-corona discharges in air, Eur. Phys. J. D 65 (3) (2011) 459–474.
[16] M. Majid, A. Rojek, H. Wiggers, P. Walzel, Visualizing electric discharges and backspray of dust layers in electrofilters, Chem. Ing. Tech. 82 (12) (2010) 2201–2207.
[17] A. Jaworek, A.T. Sobczyk, E. Rajch, Investigations of dc corona and back discharge characteristics in various gases, Electrostatics 2007 142 (012040) (2009).
[18] A. Krupa, Laboratory investigations of back discharge in multipoint-plane geometry in flue gases, J. Electrostat. 67 (2–3) (2009) 291–296.
[19] K. Hensel, Z. Machala, P. Tardiveau, Capillary microplasmas for ozone generation, Eur. Phys. J. Appl. Phys. 47 (228132) (2009).
[20] S. Sato, K. Hensel, H. Hayashi, K. Takashima, A. Mizuno, Honeycomb discharge for diesel exhaust cleaning, J. Electrostat. 67 (2–3) (2009) 77–83.
[21] W. Mista, R. Kacprzyk, Decomposition of toluene using non-thermal plasma reactor at room temperature, Catal. Today 137 (2–4) (2008) 345–349.
[22] A. Jaworek, A. Krupa, T. Czech, Back-corona generated plasma for decomposition of hydrocarbon gaseous contaminants, J. Phys. D Appl. Phys. 29 (9) (1996) 2439–2446.
[23] A. Mizuno, Electrostatic precipitation, IEEE T. Dielect. El. In. 7 (5) (2000) 615–624.
[24] K. Hensel, Y. Matsui, S. Katsura, A. Mizuno, Generation of microdischarges in porous materials, Czech. J. Phys. 54 (Part 4) (2004) C683–C689.